Louise L. Dunn,[1,2] Philippa J.L. Simpson,[1] Hamish C. Prosser,[3] Laura Lecce,[1] Gloria S.C. Yuen,[1,2] Andrew Buckle,[1] Daniel P. Sieveking,[1] Laura Z. Vanags,[3] Patrick R. Lim,[1] Renee W.Y. Chow,[1] Yuen Ting Lam,[1] Zoe Clayton,[1] Shisan Bao,[2] Michael J. Davies,[2,4] Nadina Stadler,[4] David S. Celermajer,[2,5,6] Roland Stocker,[7] Christina A. Bursill,[3] John P. Cooke,[8] and Martin K.C. Ng[1,2,6]

A Critical Role for Thioredoxin-Interacting Protein in Diabetes-Related Impairment of Angiogenesis

Impaired angiogenesis in ischemic tissue is a hallmark of diabetes. Thioredoxin-interacting protein (TXNIP) is an exquisitely glucose-sensitive gene that is overexpressed in diabetes. As TXNIP modulates the activity of the key angiogenic cytokine vascular endothelial growth factor (VEGF), we hypothesized that hyperglycemia-induced dysregulation of TXNIP may play a role in the pathogenesis of impaired angiogenesis in diabetes. In the current study, we report that high glucose–mediated overexpression of TXNIP induces a widespread impairment in endothelial cell (EC) function and survival by reducing VEGF production and sensitivity to VEGF action, findings that are rescued by silencing TXNIP with small interfering RNA. High glucose–induced EC dysfunction was recapitulated in normal glucose conditions by overexpressing either TXNIP or a TXNIP C247S mutant unable to bind thioredoxin, suggesting that TXNIP effects are largely independent of thioredoxin activity. In streptozotocin-induced diabetic mice, TXNIP knockdown to nondiabetic levels rescued diabetes-related impairment of angiogenesis, arteriogenesis, blood flow, and functional recovery in an ischemic hindlimb. These findings were associated with in vivo restoration of VEGF production to nondiabetic levels. These data implicate a critical role for TXNIP in diabetes-related impairment of ischemia-mediated angiogenesis and identify TXNIP as a potential therapeutic target for the vascular complications of diabetes.

Diabetes 2014;63:675–687 | DOI: 10.2337/db13-0417

A major part of the morbidity and mortality of diabetes arises from its vascular complications, of which impaired angiogenesis is an important feature (1). Patients with diabetes have impaired collateral development following vascular occlusion (2), poor wound healing, and increased rates of peripheral limb amputation (3). The impairment of ischemia-induced angiogenesis in diabetes is associated with reduced vascular endothelial growth factor (VEGF) production—a phenotype remedied by VEGF gene therapy (4). Monocytes isolated from diabetic individuals exhibit reduced sensitivity to the promigratory effects of VEGF, further highlighting a central role for impaired VEGF signaling in the disordered angiogenesis of diabetes (5). However, to date, the fundamental mechanisms underlying diabetes-related impairment of endothelial cell (EC) function and ischemia-mediated angiogenesis, including the role of hyperglycemia, are incompletely understood.

[1]Translational Research Group, The Heart Research Institute, Sydney, Australia
[2]Sydney Medical School, University of Sydney, Sydney, Australia
[3]Immunobiology Group, The Heart Research Institute, Sydney, Australia
[4]Free Radical Group, The Heart Research Institute, Sydney, Australia
[5]Clinical Research Group, The Heart Research Institute, Sydney, Australia
[6]Department of Cardiology, Royal Prince Alfred Hospital, Sydney, Australia
[7]Vascular Biology Division, Victor Chang Cardiac Research Institute, Sydney, Australia
[8]Department of Medicine, Stanford University School of Medicine, Stanford, CA

Corresponding author: Martin K.C. Ng, mkcng@med.usyd.edu.au.

Received 14 March 2013 and accepted 30 October 2013.

This article contains Supplementary Data online at http://diabetes.diabetesjournals.org/lookup/suppl/doi:10.2337/db13-0417/-/DC1.

Thioredoxin-interacting protein (TXNIP) is a multifunctional protein involved in the regulation of cellular homeostasis (6). TXNIP is an exquisitely glucose-inducible gene as a result of a carbohydrate response element in the promoter (7) and it is overexpressed in both diabetic animals and humans (8,9). TXNIP has been shown to reversibly bind thioredoxin-1 (TRX1), a ubiquitous oxidoreductase with antioxidant activity, in vitro (10). However, its ability to antagonize TRX1 in vivo remains unclear (11,12), and it is now appreciated that TXNIP may exert some of its effects via redox-independent mechanisms (13,14). More recently, TXNIP has been shown to bind mitochondrial thioredoxin-2 (TRX2) to induce apoptosis (15). TXNIP is increasingly implicated as a key regulator of angiogenesis (6,10). We previously identified a central role for TXNIP in VEGF-mediated EC migration, which is a key angiogenesis event (10). Indeed, the promigratory effects of angiogenic growth factors, such as VEGF, are mediated in part by their repression of TXNIP (10). We therefore hypothesized that hyperglycemia-mediated overexpression of TXNIP plays a causal role in impaired angiogenesis in diabetes.

Here, we report that elevated glucose concentrations induce a TXNIP-dependent impairment in EC function and VEGF signaling. We also demonstrate that targeted knockdown of TXNIP reverses the high glucose–induced impairment of EC angiogenic function, VEGF production, and sensitivity to VEGF action. Furthermore, we report that normalization of TXNIP expression to nondiabetic levels by small interfering RNA (siRNA) delivery in vivo rescues diabetes-related impairment of ischemia-induced angiogenesis.

RESEARCH DESIGN AND METHODS

Cell Culture and Angiogenesis Assays

Human umbilical vein ECs (HUVECs) and human coronary artery ECs (HCAECs) were cultured in MesoEndo Media (Cell Applications) in normal glucose conditions (5 mmol/L). For high glucose and mannitol conditions, media was supplemented with D-glucose to a final concentration of 15 or 25 mmol/L, or D-mannitol to a final concentration of 5 mmol/L D-glucose, 20 mmol/L D-mannitol. ECs (≤passage 4) were treated with glucose for 24 h, and then plated for migration and proliferation assays for a further 24 h in their glucose conditions. For tubulogenesis assays, ECs were pretreated with glucose for 42 h, and then assayed for a further 6 h. Therefore, ECs were exposed to glucose conditions for 48 h unless otherwise indicated.

Cell migration was assessed by a modified Boyden chamber assay with cells visualized by DAPI staining (16). Exogenous human $VEGF_{165}$ (10 ng/mL, R&D Systems) or VEGF monoclonal antibody (1 μg/mL, Sigma-Aldrich) was added where indicated. Cell proliferation was assessed by flow cytometry analysis (FC500; Beckman Coulter) of 5-ethynyl-2-deoxyuridine (EdU) incorporation (Life Technologies). Tubulogenesis on growth factor–reduced Matrigel (BD Biosciences) (16) was assessed by photomicrography and measured by tubule area. All results were confirmed by also measuring both tubule length and branch points. Nitric oxide was assessed by flow cytometry using the probe 4-amino-5-methylamino-2',7'-difluorofluorescein diacetate (DAF; Life Technologies).

Redox Assays

Total TRX activity was determined using the insulin disulfide reduction assay (17) with removal of the dithiothreitol and 70°C denaturation steps to enhance the assay's sensitivity to available TRX (18). This assay does not discriminate between TRX1 and mitochondrial TRX2, so the results are referred to as total TRX activity. Glutathione Assay Kit (BioVision) and ThioGlo-5 (Sigma-Aldrich) were used to determine reduced:oxidized glutathione (GSH:GSSG) ratios and total cellular thiols. Iron (III) and total iron were determined by electron paramagnetic resonance and inductively coupled plasma atomic emission spectroscopy, respectively (19,20).

Gene Modulation

Human TXNIP cDNA (Genbank Accession: NM_006472) or a TXNIP C247S mutant was overexpressed from the pCI-neo plasmid (Promega). Plasmid containing no insert was used as a control. Duplex siRNA to human TXNIP and a scrambled (SCR) sequence were used for in vitro gene silencing experiments (10). Plasmids and siRNA were transfected into ECs using Lipofectamine 2000 (Life Technologies). For in vivo studies, short-hairpin siRNA to murine TXNIP was expressed from pRNA-U6.1/neo (GenScript) and a SCR hairpin was used as a control.

Gene Expression

Quantitative PCR was performed using iQ SYBR-Green Supermix and iCycler Real-time PCR Detection System (Bio-Rad) and gene expression calculated using *β-actin* as a reference gene (21).

Protein Studies

Coimmunoprecipitation and Western blot analyses were performed using commercially available kits (Life Technologies). Membranes were probed for TXNIP (rabbit anti-VDUP1, 1:500; Life Technologies), TRX1 (rabbit anti-TRX1, 1:1,000; Abcam), TRX2 (rabbit anti-TRX2, 1:500; Novus Biologicals), VEGF (rabbit anti-VEGF, 1:1,000; Abcam), and endothelial nitric oxide synthase (eNOS) (mouse anti-eNOS, 1:1,000; Cell Applications). Enhanced chemiluminescence detection was performed using Quantity One (Bio-Rad) and densitometry by ImageJ software. $VEGF_{165}$, tumor necrosis factor-α, interleukin (IL)-1β, IL-8, and transforming growth factor-β were assessed by ELISA (R&D Systems). Kinase domain receptor (KDR) (VEGF receptor-2) was assessed by flow cytometry.

Apoptosis Assays

Apoptosis and necrosis were assessed after 24 h of high glucose exposure by flow cytometry analysis of Annexin-V-FITC and propidium iodide-PE staining, respectively (Sigma-Aldrich). Caspase 3/7 activation and DNA fragmentation by TUNEL assay were assessed using commercially available kits (Promega).

Diabetic Model of Murine Hindlimb Ischemia

All animal experiments were conducted with approval from the Sydney Local Health District Animal Ethics Committee. Diabetes was induced in 5-week-old male C57BL/6J mice by a bolus intraperitoneal injection of streptozotocin (STZ) (165 μg/g in citrate buffer, pH 4.5). Blood glucose levels were monitored with an Accu-Chek glucometer. At 7 weeks of age, the mice underwent unilateral hindlimb ischemia (in a subset of experiments ischemia was introduced at 13 weeks of age to assess the possibility of STZ toxicity). In brief, under methoxyflurane inhalation anesthesia, the femoral vein and superficial and deep femoral arteries were ligated with 7–0 silk sutures. The vessels were then excised down to the saphenous artery. A sham procedure was performed on the contralateral limb. Laser Doppler perfusion imaging was performed on anesthetized mice prior to surgery, post-surgery, and on days 3, 7, and 10 (moorLDI2-IR, Moor Instruments, U.K.). pRNA-U6.1/neo encoding hairpin siRNA to murine TXNIP (or SCR control) was resuspended in TransIT IN VIVO Reagent at 1 μg/μL (Mirus Bio). After imaging on days 0, 3, and 7, 50 μg of plasmid was delivered to the adductor muscle at four locations (12.5 μL/site). On days 0, 3, 7, and 10, pedal reflexes and tissue ischemia were assessed by eye (22).

Isolation of Murine Hindlimb ECs

ECs were isolated from hindlimb skeletal muscle using CD146 magnetic microbeads (Miltenyi Biotec) and their identity confirmed by von Willebrand factor (vWF) (Abcam), PECAM (Abcam), and BS1-lectin (Sigma-Aldrich) staining.

Immunohistochemistry

Adductor muscles were fixed in paraffin, sectioned, and stained to detect capillary ECs using vWF (Dako) (16) and arterioles by smooth muscle α-actin (Sigma-Aldrich). Capillary-to-myocyte ratio, arteriole-to-myocyte ratio, and vessel diameter were calculated using ImageJ software.

Statistical Analyses

All in vitro experiments were performed on at least three separate occasions using three individual EC donors, with intra-assay replicates of $n \geq 3$ for all assays (excluding ELISA, $n = 2$). All animal experiments had 8–12 mice per group, excluding the ex vivo oxidized iron analyses (5–6 per group). Experiments were analyzed using Prism 6 for Macintosh, version 6.0a software. Results are expressed as mean ± SEM. In cell experiments, two data sets were analyzed by Mann-Whitney test, three or more data sets were analyzed by Kruskal-Wallis test with Dunn multiple comparisons, and grouped data were analyzed by two-way ANOVA with Dunnett multiple comparisons. In animal experiments, data were analyzed by Mann-Whitney test, by one-way ANOVA with Holm-Sidak multiple comparisons, and in grouped data by two-way ANOVA with Holm-Sidak multiple comparisons. $P < 0.05$ was considered significant.

RESULTS

Elevated Glucose Concentration Impairs EC Function and Induces TXNIP

High glucose concentrations of 15 and 25 mmol/L were associated with dose-dependent impairment of the key endothelial functions of migration, proliferation, and tubulogenesis in HUVECs ($P < 0.05$, Fig. 1*A–C*). In parallel, increasing glucose concentrations were associated with a dose-dependent induction of *TXNIP* mRNA (Fig. 1*D*) and TXNIP protein (Fig. 1*E*). High glucose did not lead to changes in TRX1 (Fig. 1*F*) or TRX2 levels (Supplementary Fig. 1). However, high glucose conditions led to a reduction in total TRX activity ($P < 0.05$) (Fig. 1*G*), consistent with increased TXNIP expression. Similar findings were observed when HCAECs were used (Supplementary Fig. 2).

TXNIP Overexpression Mimics the Effect of High Glucose Concentrations on EC Function—an Effect That Is Independent of TRX1 Binding

To investigate if TXNIP induction alone was causal to EC dysfunction, we overexpressed TXNIP under normal glucose conditions (5 mmol/L) (Fig. 2*A*). Overexpression of wild-type or mutant TXNIP had no effect on TRX1 (Fig. 2*A*) or TRX2 levels (Supplementary Fig. 1). Overexpression of wild-type TXNIP was associated with TRX1 binding in coimmunoprecipitation assays (Fig. 2*B*) and a marked reduction in TRX activity ($P < 0.05$) (Fig. 2*C*). In contrast, overexpression of a C247S TXNIP mutant, which is unable to bind TRX1 (Fig. 2*B*) or TRX2, was not associated with any impairment in TRX activity (Fig. 2*C*). However, overexpression of either wild-type TXNIP or the C247S TXNIP mutant led to inhibition of HUVEC migration, proliferation, and tubulogenesis (Fig. 2*D–F*) comparable to the impairment seen in hyperglycemia (Fig. 1). These data suggest that TXNIP induction is sufficient to impair angiogenic processes and does so likely via a TRX-independent mechanism. Taken together with the previous results, these data indicate a key role for TXNIP in glucose-mediated EC dysfunction.

Gene Silencing of TXNIP Rescues the Impairment of Angiogenic Processes in High Glucose Conditions

To determine if we could rescue high glucose–induced impairment of EC angiogenesis, we proceeded to knockdown TXNIP in HUVEC using siRNA (Fig. 3*A*). At even the highest glucose concentration (25 mmol/L), TXNIP knockdown rescued glucose-induced impairment of

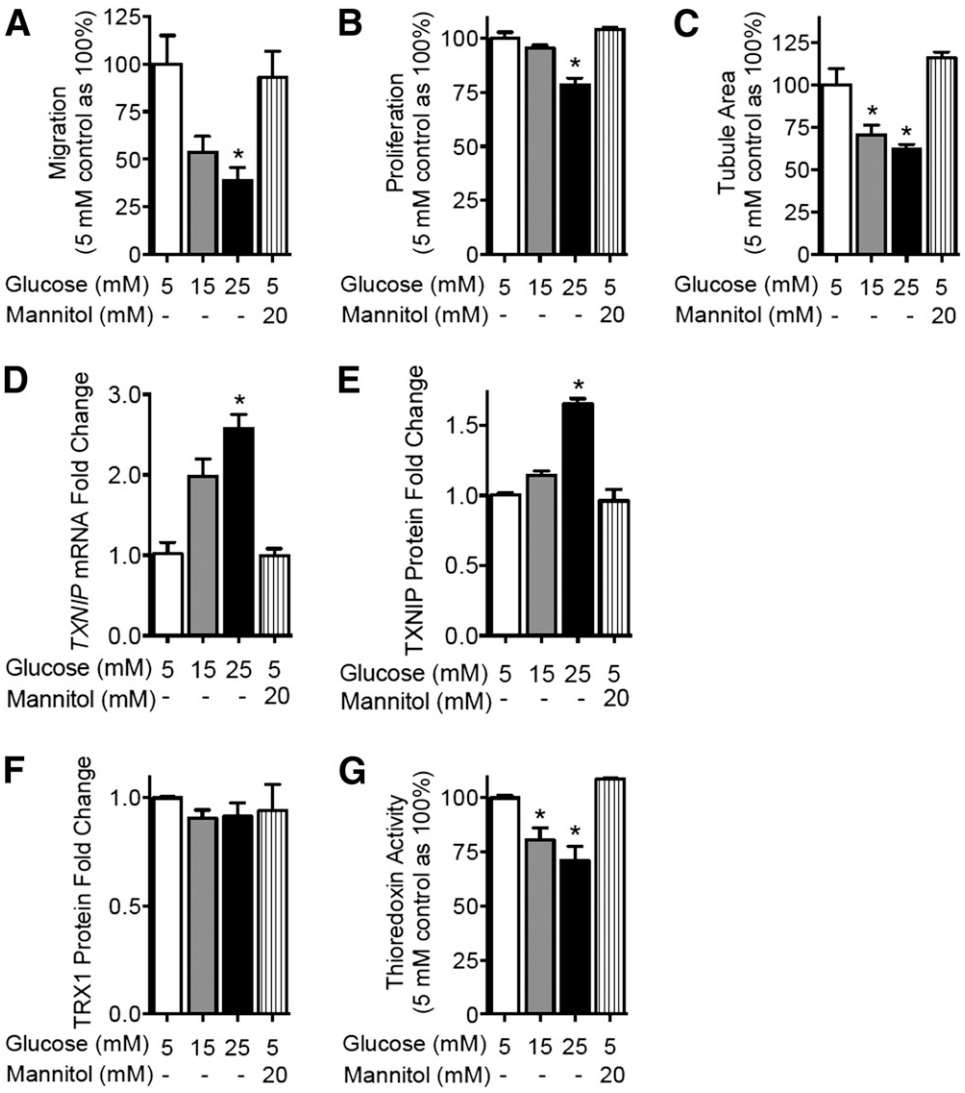

Figure 1—Elevated glucose concentration impairs EC function and induces TXNIP. HUVECs were treated with increasing glucose concentrations or an osmolar mannitol control. HUVEC angiogenic function was assessed by migration in a modified Boyden chamber assay (*A*), proliferation in an EdU incorporation assay (*B*), and tubulogenesis in a growth factor-reduced Matrigel assay (*C*). Hyperglycemic modulation of the thioredoxin system was assessed by quantitative PCR of *TXNIP* mRNA levels (*D*), Western blot analysis of TXNIP protein (*E*) and TRX1 protein (*F*), and total TRX redox activity as assessed by the insulin disulfide reduction assay (*G*). Results are representative of at least three separate experiments performed using three individual EC donors. Results are expressed as mean ± SEM and were analyzed by Kruskal-Wallis analysis with Dunn multiple comparisons. mM, mmol/L. *$P < 0.05$ compared with the 5 mM control value.

HUVEC angiogenic function, restoring migration, proliferation, and tubulogenesis to levels of control (mock-transfected HUVEC in normal 5 mmol/L glucose) (Fig. 3*B–D*). Similar results were obtained when HCAECs were assessed (Supplementary Fig. 3). These data suggest that the suppression of TXNIP can negate the inhibitory effects of hyperglycemia on EC function and therefore identify TXNIP as a potential therapeutic target for modulation of angiogenesis in the context of diabetes.

VEGF Signaling Is Impaired in Hyperglycemia and Is Restored by Gene Silencing of TXNIP

The key angiogenic cytokine VEGF has been strongly implicated in the pathogenesis of diabetes-related impairment in angiogenesis. In HUVECs, high glucose concentrations (15–25 mmol/L) were associated with a dose-dependent decrease in VEGF protein expression (Fig. 4*A*). However, gene silencing of TXNIP rescued VEGF expression and secretion to levels above that of a scrambled siRNA-treated control (Fig. 4*B–C*). Expression of KDR, the receptor mediating the proangiogenic effects of VEGF, was similarly increased by TXNIP knockdown (Fig. 4*D*). Consistent with VEGF upregulation of eNOS, TXNIP knockdown was associated with increased eNOS expression and nitric oxide production across all glucose conditions (Supplementary Fig. 4A–*C*). We also investigated whether TXNIP induction via high

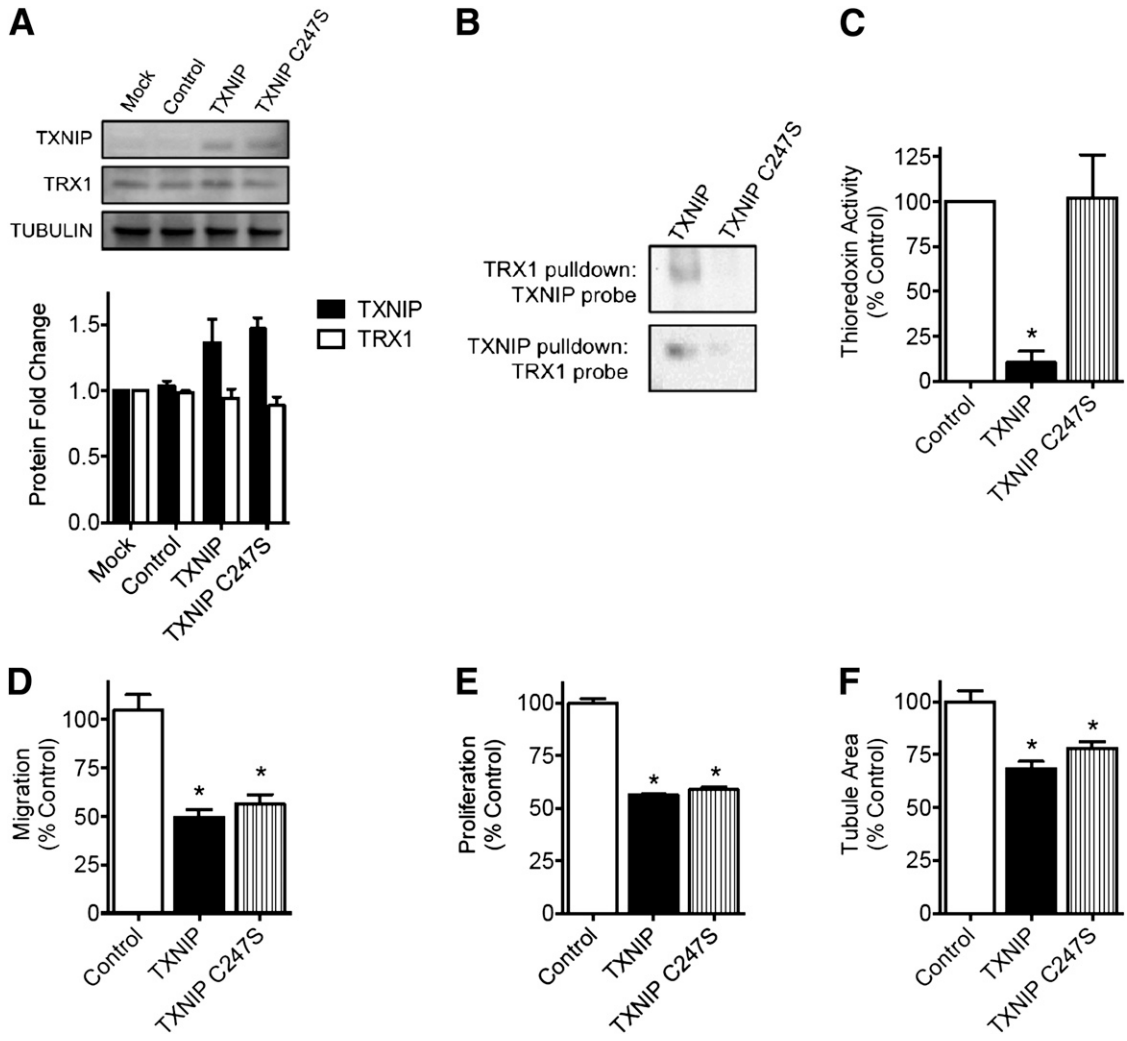

Figure 2—TXNIP overexpression replicates the deleterious effects of high glucose concentrations on EC function—an effect independent of TRX1 binding. HUVECs were transfected with plasmid encoding TXNIP, a TXNIP C247S mutant or empty plasmid (control). *A*: Western blot analysis of TXNIP and TXNIP C247S overexpression and TRX1 protein expression. *B*: Coimmunoprecipitation of TXNIP and TRX1. *C*: Total TRX redox activity in HUVEC overexpressing TXNIP, as assessed by the insulin disulfide reduction assay. HUVEC angiogenic function was assessed by migration in a modified Boyden chamber assay (*D*), proliferation in an EdU incorporation assay (*E*), and tubulogenesis in a growth factor-reduced Matrigel assay (*F*). Results are representative of at least three separate experiments performed using three individual EC donors. Results are expressed as mean ± SEM and were analyzed by Kruskal-Wallis analysis with Dunn multiple comparisons. $^*P < 0.05$ compared with control plasmid value.

glucose or TXNIP silencing affects other proangiogenic mediators, including tumor necrosis factor-α, IL-1β, transforming growth factor-β, and IL-8. We did not observe any change in these cytokine levels in response to either high glucose concentrations or TXNIP silencing (data not shown).

Impaired sensitivity to VEGF action has been reported in diabetes (5). We found that high glucose concentrations also inhibited EC sensitivity to the promigratory action of exogenous VEGF. Whereas HUVECs in 5 mmol/L glucose showed a 1.8-fold increase in migration upon the addition of exogenous VEGF, no difference is seen between cells with or without VEGF at 25 mmol/L glucose (Fig. 4*E*). However, TXNIP knockdown abrogated this impairment, with a twofold increase in migration upon the addition of VEGF being maintained across all glucose concentrations. Blocking VEGF action using a monoclonal antibody prevented all TXNIP siRNA-induced migration (Fig. 4*D–E*), confirming that the effect seen was VEGF-dependent. Similar results were obtained in HCAECs (Supplementary Fig. 4D). These data identify a key role for TXNIP in modulating VEGF-mediated angiogenesis.

EC Survival Is Impaired in Hyperglycemia and Is Restored by Gene Silencing of TXNIP

To evaluate the effect of glucose-induced TXNIP on EC survival, apoptosis was assessed in HUVECs after

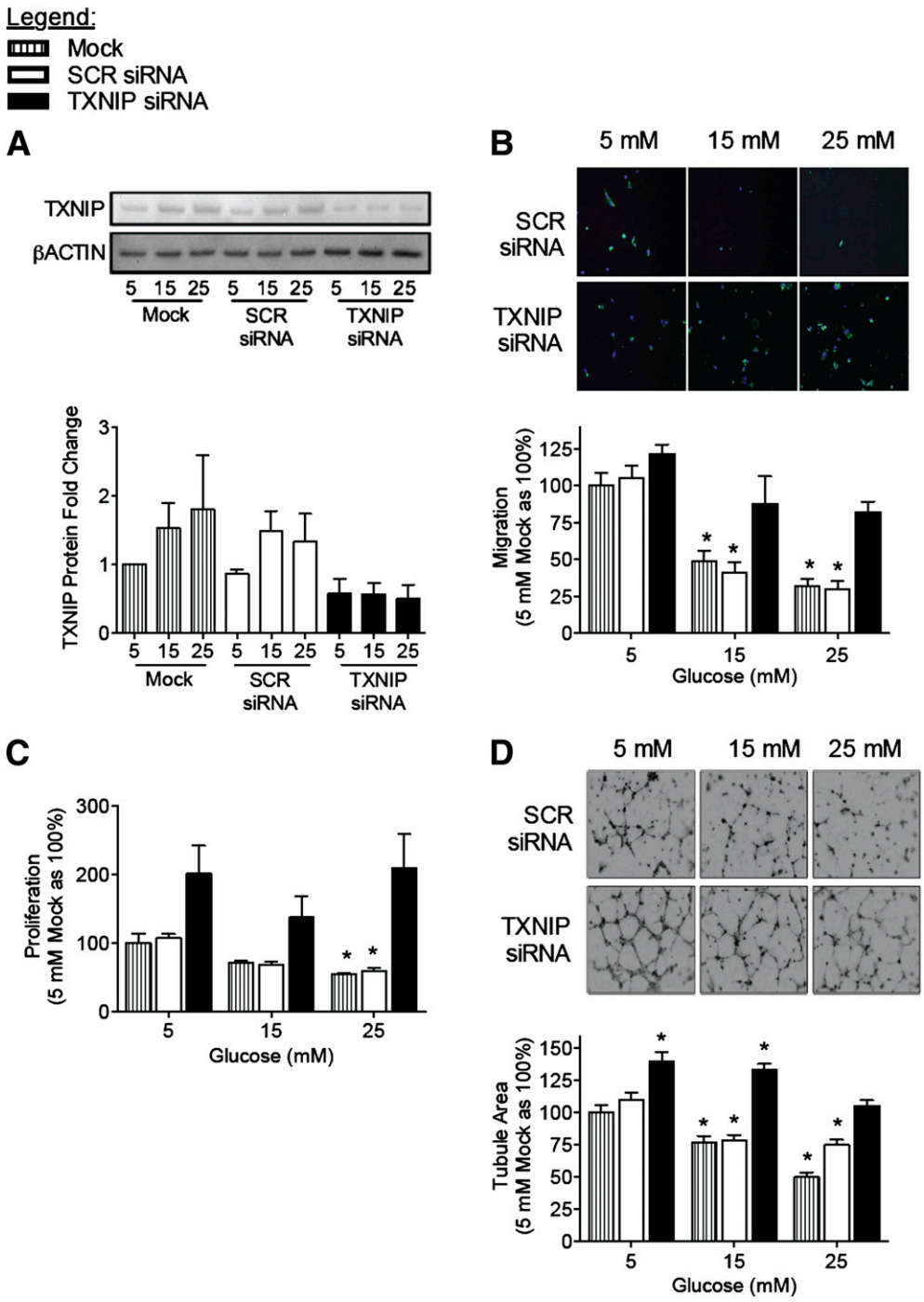

Figure 3—Gene silencing of TXNIP rescues impairment of EC function and angiogenesis induced by high glucose concentrations. HUVECs were transfected with siRNA to TXNIP (or SCR control siRNA) and then treated with 5, 15, or 25 mM (mmol/L) glucose. *A*: Western blot analysis of TXNIP expression confirms knockdown of endothelial TXNIP expression by siRNA at all glucose concentrations. Angiogenic function of siRNA-transfected, glucose-treated HUVEC was assessed by migration in a modified Boyden chamber assay (*B*), proliferation in an EdU incorporation assay (*C*), and tubulogenesis in a growth factor-reduced Matrigel assay (*D*). Representative photomicrographs were taken at 20× magnification. Results are representative of at least three separate experiments performed using three individual EC donors. Results are expressed as mean ± SEM and were analyzed by two-way ANOVA with Dunnett multiple comparisons. *$P < 0.05$ compared with 5 mM mock-transfection control.

treatment with high glucose concentrations (15–25 mmol/L). Both apoptosis, as measured by annexin-V staining, caspase 3/7 activity, and TUNEL assay of DNA fragmentation, and necrosis, as measured by propidium iodide staining, increased with glucose concentration after 24 h incubation ($P < 0.05$) (Fig. 5*A–D*). However, TXNIP knockdown by siRNA prevented high glucose–induced apoptosis (Fig. 5*A–C*) and necrosis (Fig. 5*D*).

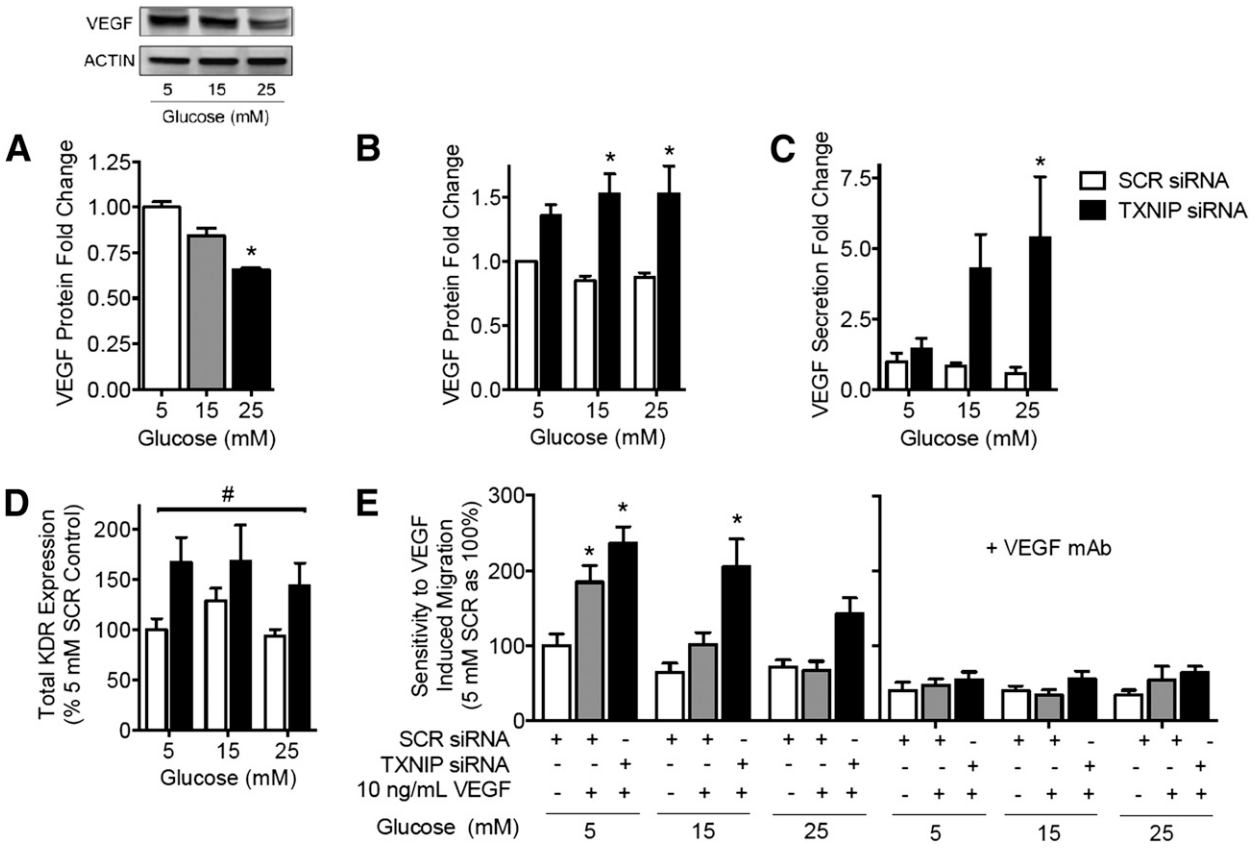

Figure 4—Gene silencing of TXNIP restores glucose-mediated impairment of both VEGF expression and sensitivity to VEGF action. *A*: HUVECs were treated with 5, 15, or 25 mM (mmol/L) glucose and analyzed for cellular VEGF by Western blot. HUVECs were transfected with siRNA to TXNIP (or SCR control siRNA) and then treated with 5, 15, or 25 mM glucose ± human $VEGF_{165}$ (10 ng/mL) ± VEGF monoclonal antibody (mAb) (1 μg/mL), as indicated, and analyzed for cellular VEGF by Western blot (*B*), secreted VEGF by ELISA of overnight growth media (*C*), and surface KDR expression by flow cytometry (*D*). *E*: VEGF-induced migration of siRNA-transfected, glucose-treated HUVEC was measured in a modified Boyden chamber assay. Results are representative of at least three separate experiments performed using three individual EC donors. Results are expressed as mean ± SEM. Results in (*A*) were analyzed by Kruskal-Wallis analysis and Dunn multiple comparisons, and in (*B–E*) by two-way ANOVA with Dunnett multiple comparisons. $^{*}P < 0.05$ compared with 5 mM control or 5 mM SCR siRNA control value, $^{\#}P < 0.05$ for TXNIP siRNA compared with SCR siRNA.

After 48 h of glucose treatment, induction of apoptosis was increasingly obscured by cell necrosis (Fig. 5*E*). Mock transfections were performed and in all cases the results were not significantly different from SCR siRNA control ($P > 0.3$, data not shown), indicating that the apoptosis and necrosis effects of high glucose and TXNIP silencing were not confounded by any adverse cellular reaction to transfection. These data link glucose-mediated induction of proapoptotic TXNIP to impairment of EC survival.

Diabetes-Related Impairment of Ischemia-Mediated Angiogenesis Is Rescued by TXNIP Silencing In Vivo

To determine if we could rescue diabetes-related impairment of ischemia-mediated angiogenesis, we elected to silence TXNIP locally using siRNA in a murine model of hindlimb ischemia. We confirmed that there were no significant changes in TXNIP expression associated with hindlimb ischemia when compared with sham-operated limbs of control mice (data not shown). At day 10, STZ-induced diabetic mice had higher blood glucose (25 ± 4 mmol/L vs.10 ± 2 mmol/L) and weighed less (19 ± 2 g vs. 23 ± 1 g) than nondiabetic controls. Diabetes was also associated with increased TXNIP expression in the hindlimb muscle ($P < 0.05$) (Fig. 6*A–B*), and this was normalized to nondiabetic levels by the intramuscular injection of TXNIP siRNA-encoding plasmid (Fig. 6*C–D*). In addition, TXNIP was specifically shown to be silenced in ECs isolated from the ischemic hindlimb (Fig. 6*E*).

Following the surgical introduction of hindlimb ischemia, diabetic mice exhibited a marked impairment of recovery compared with nondiabetic controls that was reversed by silencing TXNIP. When the mice were killed (day 10), blood flow recovery in diabetic mice was half that of controls, measured as a laser Doppler perfusion index (LDPI) (blood flow of ischemic vs. nonischemic hindlimb, 0.28 ± 0.04 vs. 0.58 ± 0.04, $P < 0.05$) (Fig. 6*F*). This observation was associated with a 40 ± 8% reduction in capillary density ($P < 0.05$) (Fig. 6*G*) and poorer pedal reflexes and tissue ischemia scores (Fig. 6*H–I*).

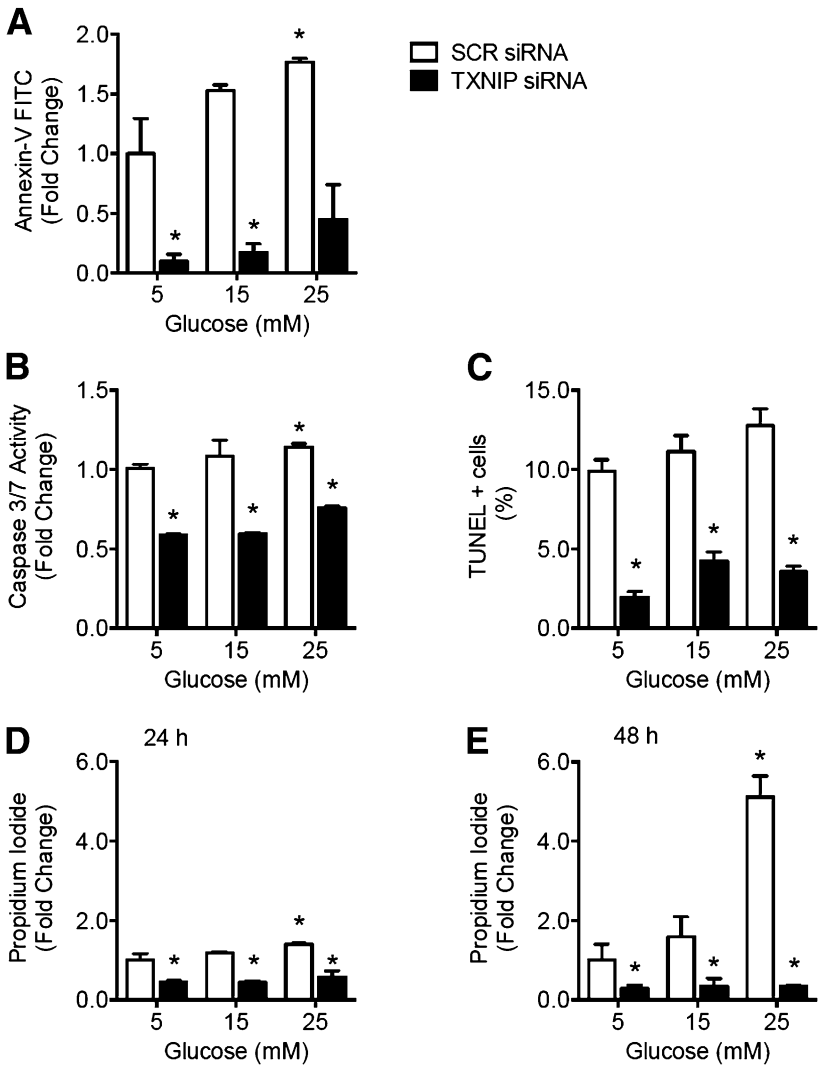

Figure 5—Glucose-mediated impairment of EC survival is rescued by gene silencing of TXNIP. HUVECs were transfected with siRNA to TXNIP (or SCR control siRNA) and then treated with 5, 15, or 25 mM (mmol/L) glucose. After 24 h of glucose treatment, apoptosis was assessed by annexin-V staining and flow cytometry analysis (*A*), caspase 3/7 activity assay (*B*), and TUNEL DNA fragmentation assay (*C*). Necrosis was assessed by propidium iodide staining and flow cytometry analysis after 24 h (*D*) and 48 h (*E*) of glucose treatment. Results are expressed as mean ± SEM and were analyzed by two-way ANOVA with Dunnett multiple comparisons. *$P < 0.05$ compared with 5 mM SCR siRNA transfected control value.

TXNIP knockdown in diabetic mice restored blood flow recovery (LDPI of 0.48 ± 0.05 at day 10) (Fig. 6*F*) and capillary density to nondiabetic control levels (Fig. 6*G*), improved diabetic pedal reflexes, and reduced tissue ischemia scores beyond control levels (Fig. 6*H–I*).

In a separate set of experiments, ischemia was surgically introduced 6 weeks after diabetes induction to rule out any effect of STZ toxicity. In agreement with the above observations, diabetic mice had elevated blood glucose and TXNIP levels (1.3-fold vs. nondiabetic controls), which was associated with impaired blood flow recovery (e.g., at day 7, 0.39 ± 0.03 vs. 0.47 ± 0.04 controls, $P < 0.05$) and capillary density (ischemic vs. nonischemic hindlimb, 0.14 ± 0.01 vs. 0.27 ± 0.02 controls, $P < 0.05$). Consistent with our initial data set, diabetic mice treated with TXNIP siRNA had improved blood flow recovery (0.45 ± 0.05) and capillary density (0.28 ± 0.02) to levels of the nondiabetic controls ($P = 0.29$ and 0.82, respectively).

Gene Silencing TXNIP In Vivo Rescues Impaired VEGF Production in Diabetes

We next examined the effects of TXNIP knockdown on VEGF expression in ischemic skeletal muscle. VEGF protein was reduced in diabetic mice compared with nondiabetic control levels ($P < 0.05$) (Fig. 6*J*). However, knockdown of TXNIP in diabetic mice restored VEGF protein to levels not statistically different from controls (Fig. 6*J*).

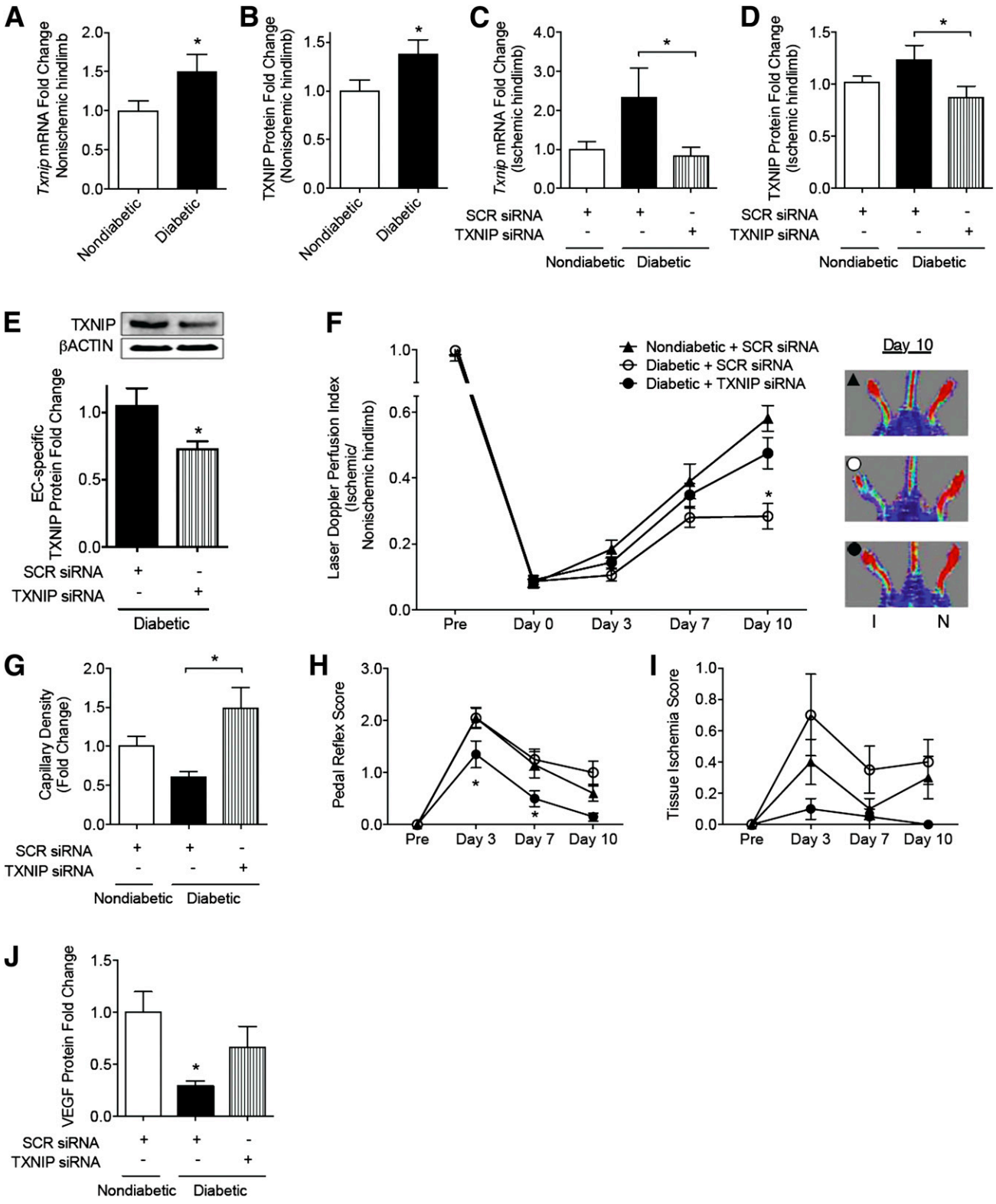

Figure 6—Diabetes-related impairment of ischemia-mediated angiogenesis is rescued by TXNIP silencing in vivo. Unilateral hindlimb ischemia was surgically introduced in nondiabetic and diabetic male C57BL/6J mice with sham preparation of the contralateral limb. Plasmid encoding siRNA to murine TXNIP was delivered by intramuscular injection. TXNIP induction and silencing was assessed in heterogeneous preparations of skeletal muscle tissue by quantitative PCR of *TXNIP* mRNA (*A*, *C*) and Western blot (*B*, *D*). *E*: ECs were isolated from hindlimb skeletal muscle tissue and assessed for TXNIP protein expression by Western blot analysis. *F*: Laser Doppler perfusion imaging was serially performed to determine the blood flow recovery; results are expressed as a ratio of blood perfusion in the ischemic versus nonischemic hindlimb. Black triangle, nondiabetic mice treated with SCR siRNA; open circle, diabetic mice treated with SCR siRNA; and black circle, diabetic mice treated with TXNIP siRNA. Images are representative of blood flow recovery at day 10. I, ischemic, N, nonischemic. *G*: Capillary density was determined by immunohistochemistry as the ratio of vWF^+ vessels per myocyte. Limb

Gene Silencing of TXNIP In Vivo Does Not Affect TRX Activity

As the role of TXNIP in modulating TRX activity in vivo remains debated (6), total TRX activity and related redox systems were assessed in hindlimb lysates. In our hindlimb ischemia model, we observed no effect of TXNIP modulation on TRX activity (Fig. 7*A*). Similarly, TXNIP knockdown had no effect on the glutathione redox ratio (GSH:GSSG), total cellular glutathione, total cellular thiols, or the proportion of oxidized iron (III) to total iron (Fig. 7*B–E*). These data indicate that the effects of TXNIP modulation in vivo may be independent of TRX redox activity and associated oxidative stress.

DISCUSSION

The vascular complications of diabetes are characterized not only by accelerated atherogenesis but also by impaired angiogenesis in response to ischemia. Despite intense scrutiny to date, the mechanisms underlying disordered EC function and angiogenesis in diabetes remain incompletely understood. The salient findings of this study are that: *1*) high levels of glucose are associated with induction of TXNIP; *2*) overexpression of TXNIP mimics the impairment in EC function observed in high glucose conditions; *3*) gene silencing of TXNIP attenuates all glucose-mediated EC angiogenic dysfunction—a finding associated with restoration of VEGF production and action; *4*) in vivo normalization of TXNIP to nondiabetic levels by siRNA rescues diabetes-related impairment of ischemia-mediated angiogenesis with restoration of VEGF production; and *5*) the effects of TXNIP on angiogenesis are, at least in part, independent of TXNIP's ability to bind to TRX1 and modulate the activity of thioredoxin. These findings demonstrate a direct link between hyperglycemia, EC dysfunction, and impaired angiogenesis via the induction of TXNIP, with particular relevance for diabetes-related impairment of ischemia-induced angiogenesis.

Extensive preclinical and clinical evidence indicates that hyperglycemia is the key driver of the vascular complications of diabetes. Intensive blood glucose control has been demonstrated to reduce diabetes-related microvascular disease (23,24). In a canine model of repeated coronary occlusions, hyperglycemia was causally linked to reduced collateral development in response to myocardial ischemia (25). Moreover, poor glycemic control in diabetic patients (HbA_{1c} >7.5%, 58.5 mmol/mol) is associated with increased ischemic complications in peripheral artery disease (26). The pathogenesis of diabetes-related impairment in ischemia-mediated angiogenesis is characterized by reduced VEGF production and attenuated sensitivity to VEGF action (4,5). However, to date, the mechanisms underpinning the impaired VEGF signaling in diabetes remains unclear. We have previously shown that TXNIP has a role in VEGF-mediated EC migration (10). As TXNIP is also induced by glucose and elevated in diabetes, we hypothesized that hyperglycemia-mediated induction of TXNIP may be a mechanism underlying the impairment of ischemia-mediated angiogenesis in diabetes.

In this study, we found that exposure to high glucose levels led to a derangement in EC angiogenic function via TXNIP induction. In agreement with previous studies, we observed that high glucose reduced VEGF production (27), and that this was accompanied by reduced EC sensitivity to the promigratory effects of VEGF. In ECs, VEGF upregulates eNOS leading to increased nitric oxide production, which induces proangiogenic events (28). However, high glucose reduces nitric oxide production and increases eNOS uncoupling (29). We found that TXNIP gene-silencing rescued high glucose–mediated impairment of eNOS levels and nitric oxide. TXNIP has been reported to facilitate the release of apoptosis signaling kinase-1 from TRX1/TRX2, which results in the initiation of apoptosis (6,15). In our studies, we found that high glucose was associated with increased apoptosis—a phenomenon that could be rescued by TXNIP gene silencing. Inhibition of apoptosis may explain, in part, some of the observed improvements, particularly in regards to proliferation and migration.

We further found that gene silencing of TXNIP rescues diabetes-related impairment of ischemia-mediated angiogenesis in a murine hindlimb ischemia model. Because TXNIP-knockout animals manifest systemic metabolic derangements that may confound angiogenesis assessment (12,18), we elected to locally knock down TXNIP by siRNA at the time of ischemia induction. TXNIP knockdown in diabetic mice rescued impairment of blood flow recovery with increases in capillary density, as well as improved pedal reflexes and reduced tissue ischemia. These results are not confounded by potential nonspecific effects of STZ toxicity as a second set of experiments carried out 6 weeks post-STZ injection recapitulated the effects of TXNIP silencing in vivo. Consistent with previous studies (4), we found reduced VEGF protein levels in the ischemic hindlimb of diabetic mice; however, TXNIP silencing restored VEGF protein levels in diabetic mice. These data are consistent with a key role

function was measured by pedal reflex score (*H*) (0 = normal; 1 = plantar but not toe flexion; 2 = no flexion; 3 = dragging of foot) and tissue ischemia score (*I*) (0 = no damage; 1 = mild discoloration; 2 = moderate discoloration). Results are representative of 8–12 mice per group and are expressed as mean ± SEM. *J*: VEGF protein expression was assessed by Western blot analysis of heterogeneous preparations of skeletal muscle tissue. Results in *A*, *B*, and *E* were analyzed by Mann-Whitney test; *C*, *D*, *G*, and *J* by one-way ANOVA with Holm-Sidak multiple comparisons; and *F*, *H*, and *I* by two-way ANOVA with Holm-Sidak multiple comparisons. *$P < 0.05$.

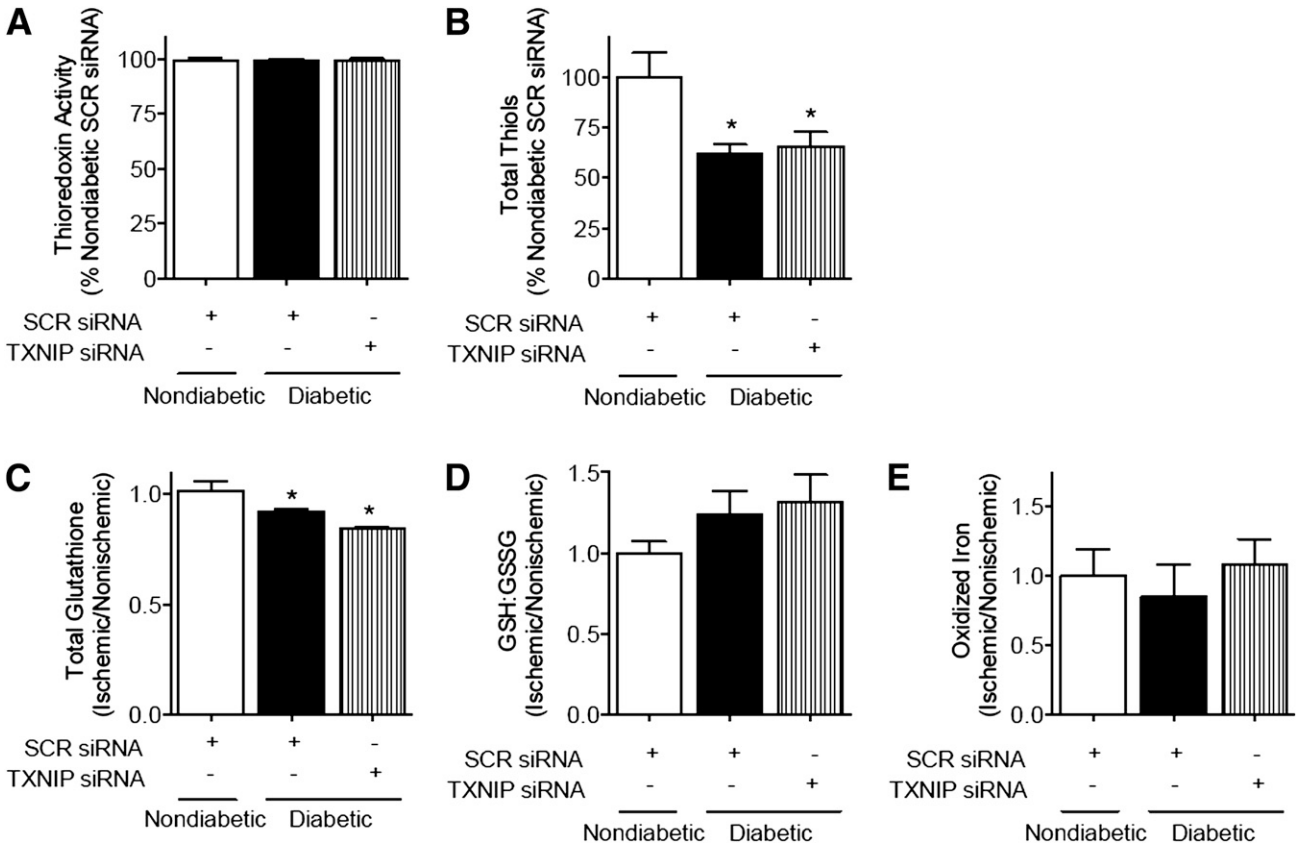

Figure 7—Gene silencing of TXNIP is not associated with detectable changes in TRX redox activity in vivo. Unilateral hindlimb ischemia was surgically introduced in nondiabetic and diabetic male C57BL/6J mice with sham preparation of the contralateral limb. Plasmid encoding siRNA to murine TXNIP was delivered by intramuscular injection. When the mice were killed, fresh adductor muscle was prepared on ice. TRX activity, as determined by the insulin disulfide reduction assay (*A*), total cellular thiols (*B*), total glutathione (*C*), GSH:GSSG ratio (*D*), and the proportion of oxidized iron to total iron (*E*) in the ischemic hindlimb were assessed in heterogeneous preparations of skeletal muscle. Results are expressed as mean ± SEM and were analyzed by one-way ANOVA with Holm-Sidak multiple comparisons. $^*P < 0.05$ to nondiabetic control.

for TXNIP in diabetes-related impairment of ischemia-mediated angiogenesis by regulation of VEGF production. It should be noted that different diabetes complications have different vascular patterns with reduced angiogenesis in ischemia and, paradoxically, increased angiogenesis in retinopathy. To date, TXNIP expression has been found to be elevated in all diabetic tissues assessed, including the retina (6,30). Indeed, TXNIP inhibition has been found to prevent inflammation and retinal injury in early stages of diabetic retinopathy (30).

Overexpression of TRX1 has been reported to enhance ischemia-mediated angiogenesis in diabetes (31). In our study, there were no differences in total TRX activity in diabetic mice compared with controls, and TXNIP knockdown had no effect on TRX activity in vivo either. Our findings in this regard are consistent with previous data from TXNIP-deficient mice that show no alterations in TRX1 activity (11,12,18). Moreover, TRX-related redox buffering systems, including the glutathione system and the reducing potential of the intracellular iron pool, were unaffected by TXNIP knockdown. Of note, regardless of siRNA treatment, diabetic mice had reduced levels of total cellular thiols compared with nondiabetic mice despite displaying no changes in total TRX activity. This may, in part, be explained by the observed reduction of total glutathione levels in diabetic mice. Our data suggest that the actions of TXNIP in vivo are, at least in part, independent of its ability to bind TRX1 or TRX2—an observation supported by our in vitro TXNIP C247S mutant experiments. However, it has recently been shown that TRX2 activity is increased in the mitochondria of myocardial cells in TXNIP knockout mice following ischemia-reperfusion injury (11), and that deletion of TRX2 is associated with impaired ischemia-mediated angiogenesis in the mouse (32). The role of mitochondrial TRX2 in diabetes-related impairment of angiogenesis in vivo was not explicitly assessed in this study and remains to be explored.

There is increasing evidence that TXNIP, a member of the arrestin domain-containing protein family that modulates G-coupled–receptor signaling (33), regulates angiogenesis. The *C*-terminal arrestin domain of TXNIP

has been shown to regulate VEGF expression in the murine lung via hypoxia inducible factor-1α, independent of TRX1 binding (13). TXNIP has also been shown to mediate nuclear export of von Hippel–Lindau protein and proangiogenic hypoxia inducible factor-1α for degradation (34). These findings support our observations that TXNIP's regulation of angiogenesis is independent of TRX1 binding. In addition to our observation that surface-expressed KDR was increased by TXNIP knockdown, it has been reported that under normal glucose conditions (5 mmol/L) the internalization of KDR following acute VEGF stimulation is reduced by TXNIP siRNA with an associated reduction in tubulogenesis (35). Interestingly, we did not observe any significant change in VEGF-stimulated EC migration with TXNIP silencing under normoglycemia. However, we found that under high glucose conditions, TXNIP siRNA strikingly rescued hyperglycemic impairment of EC migration. Cumulatively, these results indicate that TXNIP regulation of the response to VEGF may be glucose sensitive.

In conclusion, we report a direct role for the induction of TXNIP in the pathogenesis of diabetes-related impairment of angiogenesis. Gene silencing of TXNIP abrogates impairment of EC function by high glucose levels. In vivo, normalization of TXNIP expression by siRNA rescues diabetes-related impairment of ischemia-mediated angiogenesis. Interestingly, the antiangiogenic effects of TXNIP in vivo appear to be independent of inhibitory action on TRX1. Taken together, these data implicate a critical role for TXNIP in diabetes-related impairment of ischemia-induced angiogenesis and identify TXNIP as a potential therapeutic target for the vascular complications of diabetes.

Funding. This work was supported by a National Health and Medical Research Council of Australia (NHMRC) Project Grant to M.K.C.N. (512299), an NHMRC Postdoctoral Training Fellowship to L.L.D. (537537), an NHMRC Senior Principal Research Fellowship to R.S., and grants to J.P.C. from the National Institutes of Health (U01HL100397, RC2HL103400, K12HL087746) and the Tobacco-Related Disease Research Program of the University of California (18XT-0098).

Duality of Interest. No potential conflicts of interest relevant to this article were reported.

Author Contributions. L.L.D., A.B., and M.K.C.N. designed the study, designed the experiments, and interpreted the data. L.L.D., P.J.L.S., H.C.P., L.L., G.S.C.Y., A.B., D.P.S., L.Z.V., P.R.L., R.W.Y.C., Y.T.L., Z.C., S.B., D.S.C., R.S., and C.A.B. performed experiments. P.J.L.S., R.S., and M.K.C.N. contributed to data interpretation. M.J.D. and N.S. provided specific expertise. L.L.D., P.J.L.S., L.L., and M.K.C.N. wrote the manuscript. C.A.B., D.S.C., R.S., and J.P.C. reviewed and edited the manuscript. M.K.C.N. is the guarantor of this work and, as such, had full access to all the data in the study and takes responsibility for the integrity of the data and the accuracy of the data analysis.

References

1. Kannel WB, McGee DL. Diabetes and cardiovascular disease. The Framingham study. JAMA 1979;241:2035–2038
2. Abaci A, Oğuzhan A, Kahraman S, et al. Effect of diabetes mellitus on formation of coronary collateral vessels. Circulation 1999;99:2239–2242
3. Jonasson JM, Ye W, Sparén P, Apelqvist J, Nyrén O, Brismar K. Risks of nontraumatic lower-extremity amputations in patients with type 1 diabetes: a population-based cohort study in Sweden. Diabetes Care 2008;31:1536–1540
4. Rivard A, Silver M, Chen D, et al. Rescue of diabetes-related impairment of angiogenesis by intramuscular gene therapy with adeno-VEGF. Am J Pathol 1999;154:355–363
5. Waltenberger J, Lange J, Kranz A. Vascular endothelial growth factor-A-induced chemotaxis of monocytes is attenuated in patients with diabetes mellitus: A potential predictor for the individual capacity to develop collaterals. Circulation 2000;102:185–190
6. Dunn LL, Buckle AM, Cooke JP, Ng MK. The emerging role of the thioredoxin system in angiogenesis. Arterioscler Thromb Vasc Biol 2010;30:2089–2098
7. Minn AH, Hafele C, Shalev A. Thioredoxin-interacting protein is stimulated by glucose through a carbohydrate response element and induces beta-cell apoptosis. Endocrinology 2005;146:2397–2405
8. Parikh H, Carlsson E, Chutkow WA, et al. TXNIP regulates peripheral glucose metabolism in humans. PLoS Med 2007;4:e158
9. Schulze PC, Yoshioka J, Takahashi T, He Z, King GL, Lee RT. Hyperglycemia promotes oxidative stress through inhibition of thioredoxin function by thioredoxin-interacting protein. J Biol Chem 2004;279:30369–30374
10. Ng MK, Wu J, Chang E, et al. A central role for nicotinic cholinergic regulation of growth factor-induced endothelial cell migration. Arterioscler Thromb Vasc Biol 2007;27:106–112
11. Yoshioka J, Chutkow WA, Lee S, et al. Deletion of thioredoxin-interacting protein in mice impairs mitochondrial function but protects the myocardium from ischemia-reperfusion injury. J Clin Invest 2012;122:267–279
12. Yoshioka J, Imahashi K, Gabel SA, et al. Targeted deletion of thioredoxin-interacting protein regulates cardiac dysfunction in response to pressure overload. Circ Res 2007;101:1328–1338
13. Farrell MR, Rogers LK, Liu Y, Welty SE, Tipple TE. Thioredoxin-interacting protein inhibits hypoxia-inducible factor transcriptional activity. Free Radic Biol Med 2010;49:1361–1367
14. Spindel ON, World C, Berk BC. Thioredoxin interacting protein: redox dependent and independent regulatory mechanisms. Antioxid Redox Signal 2012;16:587–596
15. Saxena G, Chen J, Shalev A. Intracellular shuttling and mitochondrial function of thioredoxin-interacting protein. J Biol Chem 2010;285:3997–4005
16. Sieveking DP, Buckle A, Celermajer DS, Ng MK. Strikingly different angiogenic properties of endothelial progenitor cell subpopulations: insights from a novel human angiogenesis assay. J Am Coll Cardiol 2008;51:660–668
17. Holmgren A, Björnstedt M. Thioredoxin and thioredoxin reductase. Methods Enzymol 1995;252:199–208
18. Chutkow WA, Patwari P, Yoshioka J, Lee RT. Thioredoxin-interacting protein (Txnip) is a critical regulator of hepatic glucose production. J Biol Chem 2008;283:2397–2406
19. Sekyere EO, Dunn LL, Suryo Rahmanto Y, Richardson DR. Role of melanotransferrin in iron metabolism: studies using targeted gene disruption in vivo. Blood 2006;107:2599–2601
20. Pautsch A, Stadler N, Wissdorf O, Langkopf E, Moreth W, Streicher R. Molecular recognition of the protein phosphatase 1 glycogen targeting subunit by glycogen phosphorylase. J Biol Chem 2008;283:8913–8918

21. Pfaffl MW. A new mathematical model for relative quantification in real-time RT-PCR. Nucleic Acids Res 2001;29:e45
22. Bosch-Marce M, Okuyama H, Wesley JB, et al. Effects of aging and hypoxia-inducible factor-1 activity on angiogenic cell mobilization and recovery of perfusion after limb ischemia. Circ Res 2007;101:1310–1318
23. The Diabetes Control and Complications Trial Research Group. The effect of intensive treatment of diabetes on the development and progression of long-term complications in insulin-dependent diabetes mellitus. N Engl J Med 1993;329:977–986
24. Patel KL. Impact of tight glucose control on postoperative infection rates and wound healing in cardiac surgery patients. J Wound Ostomy Continence Nurs 2008;35:397–404; quiz 405–406
25. Basile DP, Fredrich K, Weihrauch D, Hattan N, Chilian WM. Angiostatin and matrix metalloprotease expression following ischemic acute renal failure. Am J Physiol Renal Physiol 2004;286:F893–F902
26. Selvin E, Wattanakit K, Steffes MW, Coresh J, Sharrett AR. HbA1c and peripheral arterial disease in diabetes: the Atherosclerosis Risk in Communities study. Diabetes Care 2006;29:877–882
27. Yang Z, Mo X, Gong Q, et al. Critical effect of VEGF in the process of endothelial cell apoptosis induced by high glucose. Apoptosis 2008;13:1331–1343
28. Cooke JP, Losordo DW. Nitric oxide and angiogenesis. Circulation 2002;105:2133–2135
29. Cai S, Khoo J, Channon KM. Augmented BH4 by gene transfer restores nitric oxide synthase function in hyperglycemic human endothelial cells. Cardiovasc Res 2005;65:823–831
30. Perrone L, Devi TS, Hosoya K, Terasaki T, Singh LP. Thioredoxin interacting protein (TXNIP) induces inflammation through chromatin modification in retinal capillary endothelial cells under diabetic conditions. J Cell Physiol 2009;221:262–272
31. Samuel SM, Thirunavukkarasu M, Penumathsa SV, et al. Thioredoxin-1 gene therapy enhances angiogenic signaling and reduces ventricular remodeling in infarcted myocardium of diabetic rats. Circulation 2010;121:1244–1255
32. Dai S, He Y, Zhang H, et al. Endothelial-specific expression of mitochondrial thioredoxin promotes ischemia-mediated arteriogenesis and angiogenesis. Arterioscler Thromb Vasc Biol 2009;29:495–502
33. Patwari P, Chutkow WA, Cummings K, et al. Thioredoxin-independent regulation of metabolism by the alpha-arrestin proteins. J Biol Chem 2009;284:24996–25003
34. Shin D, Jeon JH, Jeong M, et al. VDUP1 mediates nuclear export of HIF1alpha via CRM1-dependent pathway. Biochim Biophys Acta 2008;1783:838–848
35. Park SY, Shi X, Pang J, Yan C, Berk BC. Thioredoxin-interacting protein mediates sustained VEGFR2 signaling in endothelial cells required for angiogenesis. Arterioscler Thromb Vasc Biol 2013;33:737–743